PHYSICAL REVIEW D **89,** 103011 (2014)

Nonlinear variations in axisymmetric accretion

Soumyajit Bose,[1,*] Anindya Sengupta,[2,†] and Arnab K. Ray[3,‡]

[1]*Department of Physics, Indian Institute of Technology, Kanpur 208016, Uttar Pradesh, India*
[2]*Department of Physical Sciences, Indian Institute of Science Education and Research (IISER Kolkata), Mohanpur Campus, P.O. BCKV Campus Main Office, Mohanpur 741252, West Bengal, India*
[3]*Department of Physics, Jaypee University of Engineering and Technology, Raghogarh, Guna 473226, Madhya Pradesh, India*

(Received 8 April 2014; published 19 May 2014)

We subject the stationary solutions of inviscid and axially symmetric rotational accretion to a time-dependent radial perturbation, which includes nonlinearity to any arbitrary order. Regardless of the order of nonlinearity, the equation of the perturbation bears a form that is similar to the metric equation of an analogue acoustic black hole. We bring out the time dependence of the perturbation in the form of a Liénard system by requiring the perturbation to be a standing wave under the second order of nonlinearity. We perform a dynamical systems analysis of the Liénard system to reveal a saddle point in real time, whose implication is that instabilities will develop in the accreting system when the perturbation is extended into the nonlinear regime. We also model the perturbation as a high-frequency traveling wave and carry out a Wentzel-Kramers-Brillouin analysis, treating nonlinearity iteratively as a very feeble effect. Under this approach, both the amplitude and the energy flux of the perturbation exhibit growth, with the acoustic horizon segregating the regions of stability and instability.

DOI: 10.1103/PhysRevD.89.103011 PACS numbers: 98.62.Mw, 46.15.Ff, 47.10.Fg, 47.50.Gj

I. INTRODUCTION

Compressible fluids, possessing angular momentum, execute rotational motion when they are drawn into the gravitational potential well of an accretor [1]. This fact assumes particular significance when the accretor is a black hole because astrophysical black holes make their presence felt only by their strong gravitation. No direct spectral information about black holes can ever be forthcoming due to their event horizons. So evidence of black holes can only be known from the influence of their strong gravitational fields on any proximate astrophysical fluid. A system of rotational accretion onto a black hole has three principal phenomena governing the flow, namely, gravity (as implied by general relativity), transport of angular momentum, and nonlinearity. To take these up one after the other, first, when the accretor is a black hole, we concern ourselves with the physical character of curved space-time. Here we work in the spherically symmetric Schwarzschild geometry, by having recourse to what is known as a pseudo-Newtonian potential function [2–5], something that, in a Newtonian framework, mimics the salient properties of Schwarzschild space-time. We do not lose the essential effects of general relativity even in this Newtonian-like perspective [6], in which we have replaced the Schwarzschild space-time by an equivalent potential field. Apropos of gravity, another usual assumption is that the fluid is non-self-gravitating, with its flow being axisymmetric [1].

Regarding the motion of the fluid, as it drifts into the central black hole, our next concern is the centrifugal effect in the flow, which arises because test fluid elements possess angular momentum. This then brings up the question of the transport of angular momentum. Now, in a simple Newtonian treatment, the centrifugal effect will prevent a test fluid element with nonzero angular momentum from reaching the center of the potential well [6]. Relativistic theory differs on this point, in that the very strong gravity of a black hole wins against centrifugal repulsion, especially in the vicinity of the event horizon [6]. So, fluid elements with sufficient energy are able to overcome the centrifugal potential barrier and fall into the gravitating mass, whatever their angular momentum, and fluid elements with low (not merely zero) angular momentum are captured by the hole [1]. In other words, if the axisymmetric flow has low angular momentum and is driven by a very strong gravitational field (due, say, to a supermassive black hole), the radial drift will be much more conspicuous than the azimuthal drift. Now, an outward transport of angular momentum is effected through the azimuthal dynamics because of viscous shearing between two differentially rotating adjacent layers of the fluid, something that makes for a slow Keplerian infall of accreting matter into the potential well [1]. In contrast, if the angular momentum is low and the flow is highly sub-Keplerian, then the dynamics is dominated by the radial drift, suggesting that the time scale of the dynamic infall process is much smaller than the viscous time scale [7,8], which pertains to the azimuthal dynamics. In that case the

*soumyab@iitk.ac.in
†tuhin7048.sg@iiserkol.ac.in
‡arnab.kumar@juet.ac.in

viscous outward transport of angular momentum is not of much consequence, and we consider the flow inviscid. This is the underlying principle of a sub-Keplerian inviscid disc with low angular momentum [8–27]. In our study we have adopted this model, which effectively neglects the dissipation of both energy and angular momentum, thereby treating both as constants of the motion in a perfect fluid [7–9]. The accretion process purported by a conserved sub-Keplerian flow can be facilitated further if the radial velocity is significant even far away from the inner region of the disc, and on large length scales of the flow, radial velocities of such order can result, if the angular momentum is low [28–30]. Highly sub-Keplerian flows are found in detached binary systems fed by accretion from stellar winds [31,32], semidetached nonmagnetic binaries [33], and supermassive black holes fed by accretion from slowly rotating stellar clusters [34]. Also, in geometrically thick accretion discs, turbulence may produce sub-Keplerian flows [35].

Now we take up nonlinearity, which is the primary subject of our study. Mathematically, all of fluid dynamics is a nonlinear problem, and accretion flows are no exception to this rule. However, the nonlinear attribute of astrophysical accretion has not been addressed much in the literature. Here our chosen accretion model of a conserved axisymmetric flow in a pseudo-Newtonian framework allows us to focus mainly on nonlinearity by rendering the other analytical aspects of the flow simple. Nevertheless, the mathematical task remains challenging enough, involving nonlinear partial differential equations of fluid dynamics [36]. Even in the relatively simple stationary limit of these equations, we can make a case for nonlinearity. In accretion flows, the usual boundary conditions are that at large distances from the accretor, the flow is subsonic, but very close to the accretor, the flow ought to become highly supersonic, a fact borne out if the accretor is a black hole [7,37,38]. So, in the intermediate region, the bulk flow attains the speed of acoustic propagation in the fluid and becomes transonic in character. These critical conditions are the consequences of coupled first-order dynamical systems, crafted out of the equations governing stationary rotational accretion [22–24,26,27,39–41], in a classic textbook approach to nonlinear problems [42,43]. From stationary flows alone, however, we cannot fully gauge what nonlinearity implies for astrophysical accretion. So, our larger quest lies in the dynamics. In arguing for both dynamics and nonlinearity, we just need to look at the well-known nonlinear problem of the realizability of solutions passing through saddle points in a stationary phase plot. The very existence of these critical solutions is threatened by even an infinitesimal deviation from the precisely needed outer boundary condition to generate the solutions numerically [23,44]. We can, however, overcome this difficulty by a nonperturbative temporal evolution of a globally subcritical solution toward the critical state. Under qualifying approximations, such an analytical study is known [23]. Nevertheless, nonlinear problems never submit themselves easily to mathematical analyses, and there exist no analytical solutions of the fully nonlinear coupled field equations governing an accretion flow. So in the absence of any analytical formulation of the complete dynamics of the flow solutions, a tentative first step is usually a time-dependent perturbative analysis, and one such study [18] concluded that perturbations on the flow do not produce any linear mode with an amplitude that grows in time; i.e., the background solutions are marginally stable under small perturbations. The stability of inviscid sub-Keplerian flows has been studied in various ways [18,22,45], but conclusions made about stability under linearization can scarcely be extended to conditions governed by nonlinearity. Here is our attempt to bridge the gap.

First, we implement a time-dependent radial perturbation scheme on an inviscid axisymmetric accretion flow, retaining all orders of nonlinearity in the equation of the perturbation that follows. A striking feature of the equation of the perturbation is that even on accommodating nonlinearity to any arbitrary order, it conforms to the structure of the metric equation of a scalar field in Lorentzian geometry (Sec. III). This fluid analogue (an “acoustic black hole”), emulating many features of a general relativistic black hole, is a matter of continuing interest in fluid mechanics from diverse points of view [23,25,27,46–62]. Then we use the nonlinear equation of the perturbation to study the stability of globally subsonic stationary solutions under large-amplitude (nonlinear) time-dependent perturbations. Regarding the nonperturbative evolution of the accreting system, it is reasonable to suggest that the initial condition of the evolution is globally subcritical, with gravity subsequently driving the solution to a critical state, sweeping through an infinitude of intermediate subcritical states. The stability of these subcritical states is essential for a smooth temporal convergence to a stable critical state. To investigate this aspect under relatively simple nonlinear conditions, we truncate all orders of nonlinearity beyond the second order in the equation of the perturbation. Following this, we integrate out the spatial dependence of the perturbation with the help of well-defined boundary conditions on globally subcritical flows. Then we extract only the time-dependent part of the perturbation and find that it has the mathematical appearance of a Liénard system [42,43] (Sec. IV). Using standard analytical tools of dynamical systems to study the equilibrium features of this Liénard system, we show the existence of a saddle point in real time (Sec. V). This implies clearly that the stationary background solutions are unstable in time, if the perturbation is extended into the nonlinear regime. The destabilizing effect of nonlinearity remains qualitatively unaltered, when we go into the case of a high-frequency traveling-wave perturbation and carry out a Wentzel-Kramers-Brillouin (henceforth WKB) analysis (Sec. VI).

II. THE MATHEMATICAL MODEL OF THE FLOW

In models of accretion discs, imposing the condition of hydrostatic equilibrium along the vertical direction and then performing a vertical integration result in the collapse of the vertical geometry of the flow on the equatorial plane of the disc [1]. The equatorial flow is described by two coupled fields, the radial drift velocity, v, and the surface density, Σ, of which the latter is defined by vertically integrating the volume density, ρ, over the disc thickness, H.

This gives $\Sigma \cong \rho H$, and in terms of Σ, the continuity equation is [1]

$$\frac{\partial \Sigma}{\partial t} + \frac{1}{r}\frac{\partial}{\partial r}(\Sigma v r) = 0. \tag{1}$$

The axisymmetric accretion flow is driven by the gravitational field of a centrally located nonrotating black hole, but the structure of the neighboring geometry, through which the flow takes place, can still be set according to the Newtonian construct of space and time, using a pseudo-Newtonian potential [2–5]. Our principal conclusions remain qualitatively unaffected by the choice of a particular pseudo-Newtonian potential. Involving such a potential, Φ, we can give the height of the disc, under hydrostatic equilibrium in the vertical direction, as $H = \gamma^{-1/2} r (c_{\mathrm{s}}/v_{\mathrm{K}})$, with the local speed of sound, c_{s}, and the local Keplerian velocity, v_{K}, defined, respectively, by $c_{\mathrm{s}}^2 = \gamma P/\rho$ and $v_{\mathrm{K}}^2 = r(\mathrm{d}\Phi/\mathrm{d}r)$. The pressure, P, as it has been introduced in the definition of c_{s}, is expressed in terms of the volume density, ρ, by a polytropic equation of state, $P = k\rho^{\gamma}$, with γ being the polytropic exponent. In consequence of this definition of P, we note that $c_{\mathrm{s}}^2 = \partial P/\partial \rho = \gamma k \rho^{\gamma-1}$. We can also show from the first law of thermodynamics [63] that γ varies between unity (the isothermal limit) and $c_{\mathrm{P}}/c_{\mathrm{V}}$, which is the ratio of the two coefficients of specific heat capacity of a gas (corresponding to the adiabatic limit); i.e., $1 \le \gamma \le c_{\mathrm{P}}/c_{\mathrm{V}}$. So the polytropic prescription is of a much more general scope than the simple adiabatic case and is suited well for the study of open systems like astrophysical flows. Using the relationship between c_{s} and ρ, we write the disc height explicitly in terms of the standard fluid flow variables as

$$H = (\gamma k)^{1/2} \frac{\rho^{(\gamma-1)/2} r^{1/2}}{\sqrt{\gamma (\mathrm{d}\Phi/\mathrm{d}r)}}, \tag{2}$$

a result that we use to recast Eq. (1) as

$$\frac{\partial}{\partial t}[\rho^{(\gamma+1)/2}] + \frac{\sqrt{\mathrm{d}\Phi/\mathrm{d}r}}{r^{3/2}} \frac{\partial}{\partial r}\left[\frac{\rho^{(\gamma+1)/2} v r^{3/2}}{\sqrt{\mathrm{d}\Phi/\mathrm{d}r}}\right] = 0, \tag{3}$$

which is one of the two mathematical conditions governing the dynamics of the coupled fields, v and ρ.

To ascertain the second condition necessary for determining the dynamics in the radial direction, we have to first look at the dynamics along the azimuthal direction. This gives the balance of the specific angular momentum of the flow as [1]

$$\frac{\partial}{\partial t}(\Sigma r^2 \Omega) + \frac{1}{r}\frac{\partial}{\partial r}[(\Sigma v r) r^2 \Omega] = \frac{1}{2\pi r}\left(\frac{\partial \mathcal{G}}{\partial r}\right), \tag{4}$$

in which Ω is the local angular velocity of the flow. The torque, $\mathcal{G}$, on the right-hand side of the foregoing equation is to be read as $\mathcal{G} = 2\pi r \nu \Sigma r^2 (\partial \Omega/\partial r)$, with ν being the kinematic viscosity. The quantity, $r^2\Omega$, on the left-hand side of Eq. (4) is the specific angular momentum of the flow. The inviscid rotational flow of our interest can be designed as a limiting case of Eq. (4), by setting $\nu = 0$. Then, making use of Eq. (1), the comoving derivative of $r^2\Omega$, implied by the left-hand side of Eq. (4), can be made to vanish. As a result we get a simple integral solution, $r^2\Omega = \lambda$, with the constant of the motion, λ, being interpreted physically as the constant specific angular momentum of the flow. This interpretation allows us to set down the second mathematical condition of the flow along the radial direction. This is the condition of the radial momentum balance (the Euler equation), in which the centrifugal term, arising due to the rotational motion of the flow, is fixed as λ^2/r^3. After that, the radial momentum balance equation is written as

$$\frac{\partial v}{\partial t} + v\frac{\partial v}{\partial r} + \frac{1}{\rho}\frac{\partial P}{\partial r} + \frac{\mathrm{d}\Phi}{\mathrm{d}r} - \frac{\lambda^2}{r^3} = 0. \tag{5}$$

On specifying the functions, $\Phi(r)$ and P, Eqs. (3) and (5) give a complete hydrodynamic description of the axisymmetric flow in terms of the two fields, $v(r,t)$ and $\rho(r,t)$. By making explicit time dependence of these two fields disappear, i.e., by setting $\partial/\partial t \equiv 0$, we obtain the steady solutions of the flow. The resulting differential equations of the inviscid rotational flow, carrying only spatial derivatives, can be integrated to get the stationary global solutions. A noticeable feature of these stationary solutions is that they are invariant under the transformation $v \longrightarrow -v$; i.e., the mathematical problems of inflows ($v < 0$) and outflows ($v > 0$) are identical in the stationary state [23]. This invariance has adverse implications for the critical flows. Critical solutions pass through saddle points in the stationary phase portrait of the flow [22,23,44], and we can argue that generating a stationary solution through a saddle point will be practically impossible because it calls for an infinite precision in the required outer boundary condition [23,44]. Nevertheless, criticality in accretion processes is not doubted [7]. The key to resolving this paradox lies in considering explicit time dependence in the flow, because of which, as we note from Eqs. (3) and (5), the invariance under the transformation, $v \longrightarrow -v$, breaks down. Obviously then, we have to make a choice of inflows

($v < 0$) or outflows ($v > 0$) at the beginning (at $t = 0$), and solutions generated thereafter are unaffected by the difficulties associated with a saddle point in the stationary flow.

Imposing various boundary conditions on the stationary integral solutions results in various classes of flow [9,16,17]. Of these, the one of practical interest obeys the boundary conditions, $v \longrightarrow 0$ as $r \longrightarrow \infty$ (the outer boundary condition) and $v > c_{\mathrm{s}}$ at small values of r. The inner-boundary condition naturally suggests itself when it comes to accretion onto a black hole, for which, the final infall across the event horizon must be highly supersonic [7,37,38]. So an open solution that starts with a very low velocity far away from the accretor, but has to allow a fluid element to reach the accretor with supersonic speeds, must pass through a saddle point, where the flow becomes critical. When the stationary flow attains criticality, the bulk flow velocity matches the speed with which an acoustic wave can propagate through the moving compressible fluid. In the case of a polytropic and axisymmetric rotational flow, this speed is not exactly given by the sonic condition but differs slightly from it by a constant numerical factor, $\sqrt{2}(\gamma+1)^{-1/2}$, due to the geometry of the flow [18,22,23,26,27]. For a conserved flow, the critical points are either saddle points, through which open solutions pass, or they are center-type points, around which the stationary solutions form closed trajectories [22]. The solutions that pass through the saddle points may be either homoclinic or heteroclinic [9,16,17]. The number of critical points depends on the choice of the potential, $\Phi(r)$. For the simple Newtonian potential, only two critical points result [18,23], one a center-type point and the other a saddle point. In studies of axisymmetric accretion onto a black hole, however, it is an expedient practice to employ a pseudo-Newtonian potential to drive the flow. In that case, the number of critical points exceeds two, and by the properties of critical points [43], there are multiple saddle points. Since open critical solutions, connecting the outer boundary of the flow to the event horizon of a black hole, have to pass through saddle points, an inflow process that is made to traverse all of these saddle points is multicritical [7–9,11–13,15,16,19–21,25,39]. In such a flow, a fluid element reaches the accretor after having traveled through more than one saddle point, and in between two successive saddle points, the flow suffers a shock [9–12,15–17,21,25]. It is at the discontinuity of a shock that a solution is demoted from its supercritical state to a subcritical one, following which the solution has to regain supercriticality by traveling through another saddle point [9,16,17].

Thus far, we have looked at the properties of the accretion flow from a stationary perspective, which is relatively easy to follow. It is the dynamics of the flow that poses a mathematical problem of greater complexity. In comparatively simple studies involving time dependence [18,22], the inviscid and axisymmetric flow is found to be stable under the effect of linearized perturbations. This, however, does not say much about the nonperturbative temporal evolution of the velocity and density fields. In such a mathematical problem, we have to work with a coupled set of nonlinear partial differential equations, as implied by Eqs. (3) and (5), but no analytical solutions exist for these coupled dynamic nonlinear equations. Now, the nonperturbative dynamic evolution of global $v(r,t)$ and $\rho(r,t)$ profiles is crucial in generating the critical flow. It is the way in which the two fields evolve vis-à-vis each other that determines if the critical state would be achieved or not. We can envisage the dynamic process as one in which initially the velocity field, $v(r,t)$, is subcritical and nearly uniform for all values of r, in the absence of any driving force. Then with the introduction of a gravitational field (at $t = 0$), about whose center, the fluid distribution may randomly possess some net angular momentum, the hydrodynamic fields, v and ρ, start evolving in time. In the regions where the temporal growth of v outpaces the temporal growth of ρ (to which c_{s} is connected) and gravity (given by r^{-2}) dominates the inhibitive centrifugal effects of rotation (given by r^{-3}), the infall process becomes supercritical. Otherwise, it continues to remain subcritical. Under the approximation of a "pressureless" motion of a fluid in a gravitational field [64], qualified support for attaining criticality has come from a nonperturbative dynamic perspective [23], guided by the criterion that the total specific mechanical energy at the end of the evolution would be the same as what it was at the start of the evolution.

III. NONLINEARITY IN THE PERTURBATIVE ANALYSIS

Equations (3) and (5) are integrated in their stationary limits, to obtain the spatial profiles, $v \equiv v_0(r)$ and $\rho \equiv \rho_0(r)$. A standard method of perturbative analysis is to apply small (to a linear order) time-dependent radial perturbations on the stationary solutions, $v_0(r)$ and $\rho_0(r)$. By this, however, we do not gain much insight into the time-dependent evolutionary aspects of the hydrodynamic flow. Our next logical act, therefore, is to incorporate nonlinearity in the perturbative method. With the inclusion of nonlinearity in progressively higher orders, the perturbative analysis incrementally approaches the actual time-dependent evolution of the global solutions, after it has started with a given stationary profile at $t = 0$ (it makes physical sense to suggest that this initial profile is spatially subcritical over the entire flow domain).

We prescribe the perturbation as $v(r,t) = v_0(r) + v'(r,t)$ and $\rho(r,t) = \rho_0(r) + \rho'(r,t)$, in which the primed quantities indicate a perturbation about a stationary background. We define a new variable, $f(r,t) = \rho^{(\gamma+1)/2} v r^{3/2} / \sqrt{\mathrm{d}\Phi/\mathrm{d}r}$, following a mathematical procedure employed previously in studies on inviscid axisymmetric accretion [18,22,23]. We can see that this variable emerges as a constant of the motion from the stationary limit of Eq. (3), and this constant, f_0, can be identified closely with the matter flow rate, within a fixed geometrical factor. In terms of v_0 and ρ_0, we can write this constant $f_0 = \rho_0^{(\gamma+1)/2} v_0 r^{3/2}/\sqrt{\mathrm{d}\Phi/\mathrm{d}r}$. On applying the perturbation scheme for v and ρ, the perturbation in f, without losing anything of nonlinearity, is derived as

$$\frac{f'}{f_0} = \frac{\zeta}{\beta^2}\frac{\rho'}{\rho_0} + \frac{v'}{v_0} + \frac{\zeta}{\beta^2}\frac{\rho'}{\rho_0}\frac{v'}{v_0}, \tag{6}$$

in which,

$$\zeta = 1 + \frac{1}{1\cdot 2}\left(\frac{\gamma-1}{2}\right)\frac{\rho'}{\rho_0} + \frac{1}{1\cdot 2\cdot 3}\left(\frac{\gamma-1}{2}\right)\left(\frac{\gamma-3}{2}\right)\left(\frac{\rho'}{\rho_0}\right)^2 + \cdots, \tag{7}$$

and $\beta = \sqrt{2}(\gamma+1)^{-1/2}$. Equation (6) connects the perturbed quantities, v', ρ', and f' to one another. To get a relation between ρ' and f' only, we take Eq. (3) and apply the perturbation scheme on it. This results in

$$\frac{\partial}{\partial t}\left(\frac{\zeta}{\beta^2}\frac{\rho'}{\rho_0}\right) = -v_0\frac{\partial}{\partial r}\left(\frac{f'}{f_0}\right). \tag{8}$$

To obtain a similar relationship solely between v' and f', we combine the conditions given by Eqs. (6) and (8) to get

$$\frac{\partial v'}{\partial t} = \frac{v}{f}\left(\frac{\partial f'}{\partial t} + v\frac{\partial f'}{\partial r}\right). \tag{9}$$

We stress at this point that in Eqs. (6), (8), and (9) all orders of nonlinearity have been maintained. Now returning to Eq. (3) and taking its partial time derivative, an alternative form of the perturbation on the continuity condition appears as

$$\frac{1}{\rho}\frac{\partial\rho'}{\partial t} = -\frac{\beta^2 v}{f}\left(\frac{\partial f'}{\partial r}\right). \tag{10}$$

Equations (8) and (10) are equivalent expressions of the same principle, but its two distinct mathematical forms arise due to the axial symmetry of the flow, a feature that does not occur in spherical symmetry [62]. Of the two forms, Eq. (10) is more useful than Eq. (8), when we take the second-order partial time derivative of Eq. (5), and use the perturbation scheme on it to obtain

$$\frac{\partial^2 v'}{\partial t^2} + \frac{\partial}{\partial r}\left(v\frac{\partial v'}{\partial t} + \frac{c_s^2}{\rho}\frac{\partial\rho'}{\partial t}\right) = 0. \tag{11}$$

We note the importance of using Eq. (10) in arriving at Eq. (11), which has the appearance of a similar equation of a nonlinear perturbation in the case of spherical symmetry [62]. We exploit this similarity and apply all of the mathematical methods of the spherically symmetric problem [62] to our present problem of a rotational flow. This is a crucial advantage.

Now making use of Eq. (9), its second-order partial time derivative, and Eq. (10) we derive a fully nonlinear equation of the perturbation from Eq. (11), running in a symmetric form as

$$\frac{\partial}{\partial t}\left(h^{tt}\frac{\partial f'}{\partial t}\right) + \frac{\partial}{\partial t}\left(h^{tr}\frac{\partial f'}{\partial r}\right) + \frac{\partial}{\partial r}\left(h^{rt}\frac{\partial f'}{\partial t}\right) + \frac{\partial}{\partial r}\left(h^{rr}\frac{\partial f'}{\partial r}\right) = 0, \tag{12}$$

in which,

$$h^{tt} = \frac{v}{f}, \quad h^{tr} = h^{rt} = \frac{v^2}{f}, \quad h^{rr} = \frac{v}{f}(v^2 - \beta^2 c_s^2). \tag{13}$$

Going by the symmetry of Eq. (12), we can recast it in a compact form as

$$\partial_\mu(h^{\mu\nu}\partial_\nu f') = 0, \tag{14}$$

with the Greek indices running from 0 to 1, under the equivalence that 0 stands for t and 1 stands for r. The derivation of Eq. (14) is pertinent to any kind of stationary background solution, with the only restriction being that the perturbation is radial. Further, Eq. (14), or equivalently, Eq. (12), is a nonlinear equation containing arbitrary orders of nonlinearity in the perturbative expansion. All of the nonlinearity is carried in the metric elements, $h^{\mu\nu}$. If we were to have worked with a linearized equation, then $h^{\mu\nu}$ could be read from the matrix [22,23],

$$h^{\mu\nu} = \frac{v_0}{f_0}\begin{pmatrix} 1 & v_0 \\ v_0 & v_0^2 - \beta^2 c_{s0}^2 \end{pmatrix}, \tag{15}$$

in which $c_{s0} \equiv c_{s0}(r)$ is the steady-state value of the local speed of sound.

Now, in Lorentzian geometry, the d'Alembertian for a scalar field in curved space is expressed in terms of the metric, $g_{\mu\nu}$, as

$$\Delta\varphi \equiv \frac{1}{\sqrt{-g}}\partial_\mu(\sqrt{-g}g^{\mu\nu}\partial_\nu\varphi), \tag{16}$$

with $g^{\mu\nu}$ being the inverse of the matrix implied by $g_{\mu\nu}$ [49,59]. Comparing Eqs. (14) and (16) with each other, we look for an equivalence between $h^{\mu\nu}$ and $\sqrt{-g}g^{\mu\nu}$. Clearly, Eq. (14) gives an expression for f' that is of the type given by Eq. (16). We extract the metrical part of Eq. (14) in the linear order, and the inverse of this metric implies an acoustic horizon, when $v_0^2 = \beta^2 c_{s0}^2$. This approach is equivalent to the way in which an analogue metric can be fashioned out of a potential flow by converting its velocity field into the gradient of a scalar function and then by perturbing the scalar function [25,49,50,59]. In contrast to this method of exploiting the potential character of the flow, our derivation of Eq. (14) makes use of the continuity condition. We argue that the latter method is more comprehensive because the continuity condition is based on matter conservation, which is a more forceful conservation principle than that of energy conservation (especially concerning open astrophysical flows), on which the scalar-potential approach is founded. If the flow were to have contained mechanisms for dissipation (as it is happens in models of axisymmetric accretion), then the potential-flow method would have been ineffective, but our method of making use of the matter conservation principle would still have delivered an equation of the perturbation.

A remarkable result of our analysis is that regardless of the order of nonlinearity that we may retain the symmetric form of the Lorentzian metric equation remains unchanged, as we can see from Eq. (14). The preservation of this symmetry under arbitrary orders of nonlinearity is also exhibited in various other fluid systems like the hydraulic jump flow [55], the spherically symmetric outflows of nuclear matter [61], and the spherically symmetric inflows of astrophysical matter [62]. While the analogue metric holds its ground in spite of nonlinearity, a serious consequence of including nonlinearity in the mathematical treatment is to compromise the notion of a static acoustic horizon in the flow. This is because a zero-order description of $h^{\mu\nu}$, coming from Eq. (15), is no longer adequate. Instead, the elements, $h^{\mu\nu}$, are to be defined by Eq. (13), which carries time dependence in the higher nonlinear orders. This point of view agrees with a numerical study carried out by [58], who showed that sonic horizons would move about their static positions under strong perturbations, and the analogy between a sonic horizon and the event horizon of a black hole would appear limited. So the close correspondence between the physics of acoustic flows and many features of black hole physics is valid only in the linear order.

IV. STANDING WAVES ON SUBCRITICAL INFLOWS

All physically relevant stationary inflow solutions obey the outer boundary condition, $v(r) \longrightarrow 0$ as $r \longrightarrow \infty$. Among these solutions, a critical inflow will reach the accretor with a high super-critical speed, but somewhere along the way, this flow will also undergo a discontinuity due to a shock. So critical inflows are highly subcritical at the outer boundary, are highly supercritical near the accretor (the inner boundary), and have a discontinuity in the interim region [9,16,17]. There is, however, an entire class of inflow solutions that are globally subcritical, conforming to the inner boundary condition, $v(r) \longrightarrow 0$ as $r \longrightarrow 0$. For a gravity-driven evolution of an inflow solution to a critical state, the initial state of the evolution, as well as the intermediate states in the progression toward criticality, should realistically be subcritical. So the stability of globally subcritical flows has a significant bearing on how a critical solution will evolve eventually. Imposing an Eulerian perturbation on these subcritical inflows, their stability was studied under a linearized regime, and the amplitude of the perturbation, which was modeled as a standing wave, was seen to maintain a constant profile in time [18]. In this respect we may say that the subcritical states are marginally stable. However, we have to be cautious in extending this argument when we consider nonlinearity in the perturbative effects, as it rightly ought to be done in a fluid flow problem.

Equation (12) gives a nonlinear equation of the perturbation, accommodating nonlinearity to any desired order. We design the perturbation to behave like a standing wave about a globally subcritical stationary solution, obeying the boundary condition that the spatial part of the perturbation vanishes at two radial points in the axisymmetric geometry, one at a great distance from the accretor (the outer boundary) and the other very close to it (the inner boundary). While the former boundary is a self-evident fact of the flow, there is a certain measure of difficulty in identifying the latter. The guiding principle behind the choice of the two boundaries is that the background stationary solution should be continuous in the interim region. For a globally continuous subcritical solution that connects the outer boundary to the accretor, the inner boundary is obviously the surface of the accretor itself. If, however, even a subcritical inflow is disrupted by a shock, then the inner boundary should be the standing front of the shock itself. It is conceivable that no part of the perturbation on the background flow may percolate through the shock front, and so, the discontinuous front itself may be set as a boundary for the perturbation. Such piecewise continuity of a stability analysis, on either side of a discontinuity, is not uncommon in studies on fluid flows [55].

Our mathematical treatment involving nonlinearity is confined to the second order only (the lowest order of nonlinearity). Even simplified so, the entire procedure carries much of the complications associated with a nonlinear problem. The restriction of not going beyond the second order of nonlinearity implies that $h^{\mu\nu}$ in Eq. (13) will contain primed quantities in their first power only. Taken together with Eq. (12), this will preserve all of the terms that are nonlinear in the second order. So, performing the necessary expansion of $v = v_0 + v'$, $\rho = \rho_0 + \rho'$ and $f = f_0 + f'$ in Eq. (13), up to the first order only, and defining a new set of metric elements, $q^{\mu\nu} = f_0 h^{\mu\nu}$, we obtain

$$\partial_\mu (q^{\mu\nu} \partial_\nu f') = 0, \tag{17}$$

in which μ and ν are to be read just as in Eq. (14). The elements, $q^{\mu\nu}$, in Eq. (17) carry all the three perturbed quantities, ρ', v', and f'. Our next task is to substitute both ρ' and v' in terms of f' since Eq. (17) is over f' only. To make this substitution possible, first we have to use Eq. (6) to close v' in terms of ρ' and f' in all $q^{\mu\nu}$. While doing so, we ignore the product term of ρ' and v' in Eq. (6) because including it will raise Eq. (17) to the third order of nonlinearity. By the same token, we also have to take $\zeta = 1$ in Eq. (7). Once v' has been substituted in this manner, we write ρ' in terms of f' by invoking Eq. (8), with the reasoning that if ρ' and f' are both multiplicatively separable functions of space and time, with an exponential time part (all of which are standard prescriptions in any mathematical treatment on standing waves), then

$$\frac{1}{\beta^2}\frac{\rho'}{\rho_0} = \sigma(r)\frac{f'}{f_0}, \tag{18}$$

with σ being a function of r only, a fact that simplifies much of the calculations to follow. The exact functional form of $\sigma(r)$ is determined from the way the spatial part of f' is prescribed, but on general physical grounds we reason that when ρ', v', and f' are all real fluctuations, σ should likewise be real. We shall corroborate this argument independently in Sec. VI, but now we express the elements, $q^{\mu\nu}$, in Eq. (17), entirely in terms of f' as

$$q^{tt} = v_0\left(1 + \epsilon\xi^{tt}\frac{f'}{f_0}\right), \qquad q^{tr} = v_0^2\left(1 + \epsilon\xi^{tr}\frac{f'}{f_0}\right),$$
$$q^{rt} = v_0^2\left(1 + \epsilon\xi^{rt}\frac{f'}{f_0}\right),$$
$$q^{rr} = v_0(v_0^2 - \beta^2 c_{s0}^2) + \epsilon v_0^3\xi^{rr}\frac{f'}{f_0}, \tag{19}$$

in all of which, ϵ has been introduced as a nonlinear "switch" parameter to track all the nonlinear terms. When $\epsilon = 0$, only linearity remains, and in this limit we converge to the familiar linear result implied by Eq. (15). In the opposite extreme, when $\epsilon = 1$, in addition to the linear effects, the lowest order of nonlinearity (the second order) becomes activated in Eq. (17), and the linearized stationary conditions of a sonic horizon get disturbed due to the nonlinear ϵ-dependent terms. This very feature was observed numerically by [58]. Equation (19) also contains the factors, $\xi^{\mu\nu}$, all of which read as

$$\xi^{tt} = -\sigma, \qquad \xi^{tr} = \xi^{rt} = 1 - 2\sigma,$$
$$\xi^{rr} = 2 - \sigma\left[3 + \left(\frac{\gamma - 3}{\gamma + 1}\right)\frac{\beta^2 c_{s0}^2}{v_0^2}\right]. \tag{20}$$

Taking Eqs. (17), (19), and (20) together, we finally obtain a nonlinear equation of the perturbation, completed up to the second order, without the loss of any relevant term.

To render Eq. (17) into a workable form, we first expand it in full and then divide it throughout by v_0. In doing so, we also exploit the symmetry afforded by $\xi^{tr} = \xi^{rt}$. The desirable form of the equation of the perturbation should be such that its leading term would be a second-order partial time derivative of f', with unity as its coefficient. To arrive at this form, an intermediate step will involve a division by $1 + \epsilon\xi^{tt}(f'/f_0)$, which, binomially, is the equivalent of a multiplication by $1 - \epsilon\xi^{tt}(f'/f_0)$, with a truncation applied thereafter. This is dictated by the simple principle that to keep only the second-order nonlinear terms, it will suffice to retain just those terms which carry ϵ in its first power. The result of this entire exercise is

$$\frac{\partial^2 f'}{\partial t^2} + 2\frac{\partial}{\partial r}\left(v_0\frac{\partial f'}{\partial t}\right) + \frac{1}{v_0}\frac{\partial}{\partial r}\left[v_0(v_0^2 - \beta^2 c_{s0}^2)\frac{\partial f'}{\partial r}\right]$$
$$+ \frac{\epsilon}{f_0}\left\{\xi^{tt}\left(\frac{\partial f'}{\partial t}\right)^2 + \frac{\partial}{\partial r}\left(\xi^{rt}v_0\frac{\partial f'^2}{\partial t}\right) - \frac{v_0}{2}\frac{\partial \xi^{rt}}{\partial r}\frac{\partial f'^2}{\partial t}\right.$$
$$+ \frac{1}{2v_0}\frac{\partial}{\partial r}\left(\xi^{rr}v_0^3\frac{\partial f'^2}{\partial r}\right) - 2\xi^{tt}f'\frac{\partial}{\partial r}\left(v_0\frac{\partial f'}{\partial t}\right)$$
$$\left. - \frac{\xi^{tt}f'}{v_0}\frac{\partial}{\partial r}\left[v_0(v_0^2 - \beta^2 c_{s0}^2)\frac{\partial f'}{\partial r}\right]\right\} = 0, \tag{21}$$

in which, setting $\epsilon = 0$, what remains is the linear equation discussed in some earlier works [18,22]. We use a solution, $f'(r,t) = R(r)\phi(t)$, in Eq. (21), with R being a real function [65]. Then we multiply the resulting expression throughout by $v_0 R$ and perform some algebraic simplifications by partial integrations to finally get

$$\ddot{\phi}v_0R^2 + \dot{\phi}\frac{\mathrm{d}}{\mathrm{d}r}(v_0R)^2 + \phi\left\{\frac{\mathrm{d}}{\mathrm{d}r}\left[\frac{v_0}{2}(v_0^2 - \beta^2 c_{s0}^2)\frac{\mathrm{d}R^2}{\mathrm{d}r}\right]\right.$$
$$\left. - v_0(v_0^2 - \beta^2 c_{s0}^2)\left(\frac{\mathrm{d}R}{\mathrm{d}r}\right)^2\right\} + \frac{\epsilon}{f_0}\left[\dot{\phi}^2\xi^{tt}v_0R^3\right.$$
$$+ \dot{\phi}\phi\left[\frac{\mathrm{d}}{\mathrm{d}r}(\xi^{rt}v_0^2R^3) + \xi^{rt}\frac{v_0^2}{3}\frac{\mathrm{d}R^3}{\mathrm{d}r} - \xi^{tt}R\frac{\mathrm{d}}{\mathrm{d}r}(v_0R)^2\right]$$
$$+ \phi^2\left\{v_0(v_0^2 - \beta^2 c_{s0}^2)\frac{\mathrm{d}R}{\mathrm{d}r}\frac{\mathrm{d}}{\mathrm{d}r}(\xi^{tt}R^2) - \xi^{rr}v_0^3R\left(\frac{\mathrm{d}R}{\mathrm{d}r}\right)^2\right.$$
$$\left.\left. - \frac{\mathrm{d}}{\mathrm{d}r}\left[\xi^{tt}\frac{v_0}{3}(v_0^2 - \beta^2 c_{s0}^2)\frac{\mathrm{d}R^3}{\mathrm{d}r}\right] + \frac{\mathrm{d}}{\mathrm{d}r}\left(\xi^{rr}\frac{v_0^3}{3}\frac{\mathrm{d}R^3}{\mathrm{d}r}\right)\right\}\right] = 0, \tag{22}$$

in which the overdots indicate full derivatives in time. We integrate all spatial dependence out of Eq. (22) by using two boundary conditions, one very far from the accretor (at the outer boundary) and the other one (at the inner boundary) either very close to the accretor or at a standing shock front where the background solution becomes discontinuous. At both of these boundary points, we constrain the perturbation to have a vanishing amplitude in time, while the background solution maintains a continuity in the interim region. The boundary conditions ensure that all of the "surface" terms of the integrals in

Eq. (22) will vanish (which is the reason for the tedious mathematical exercise to extract several "surface" terms). So after carrying out the required integration on Eq. (22), over the entire region trapped between the two specified boundaries, all that survives is the purely time-dependent equation, having the form,

$$\ddot{\phi} + \epsilon(\mathcal{A}\phi + \mathcal{B}\dot{\phi})\dot{\phi} + \mathcal{C}\phi + \epsilon\mathcal{D}\phi^2 = 0, \tag{23}$$

in which the constants, $\mathcal{A}$, $\mathcal{B}$, $\mathcal{C}$, and $\mathcal{D}$, are to be read as

$$\begin{aligned}
\mathcal{A} &= \frac{1}{f_0}\left(\int v_0 R^2 \mathrm{d}r\right)^{-1}\int\left[\xi^{rt}\frac{v_0^2}{3}\frac{\mathrm{d}R^3}{\mathrm{d}r} - \xi^{tt}R\frac{\mathrm{d}}{\mathrm{d}r}(v_0 R)^2\right]\mathrm{d}r,\\
\mathcal{B} &= \frac{1}{f_0}\left(\int v_0 R^2 \mathrm{d}r\right)^{-1}\int \xi^{tt} v_0 R^3 \mathrm{d}r,\\
\mathcal{C} &= -\left(\int v_0 R^2 \mathrm{d}r\right)^{-1}\int v_0(v_0^2 - \beta^2 c_{s0}^2)\left(\frac{\mathrm{d}R}{\mathrm{d}r}\right)^2\mathrm{d}r,\\
\mathcal{D} &= \frac{1}{f_0}\left(\int v_0 R^2 \mathrm{d}r\right)^{-1}\int\left[v_0(v_0^2 - \beta^2 c_{s0}^2)\frac{\mathrm{d}R}{\mathrm{d}r}\frac{\mathrm{d}}{\mathrm{d}r}(\xi^{tt}R^2)\right.\\
&\qquad \left. - \xi^{rr} v_0^3 R\left(\frac{\mathrm{d}R}{\mathrm{d}r}\right)^2\right]\mathrm{d}r,
\end{aligned} \tag{24}$$

respectively. The form in which we have abstracted Eq. (23) is that of a general Liénard system [42,43]. All of the terms in Eq. (23), bearing the parameter, ϵ, have arisen in consequence of nonlinearity. Setting $\epsilon = 0$, we do readily regain the known linear results [18], but to understand the role of nonlinearity in the perturbation, we have to look into the fully nonlinear import of the Liénard system in Eq. (23).

V. EQUILIBRIUM CONDITIONS IN THE LIÉNARD SYSTEM

The mathematical form of a Liénard system is that of a damped nonlinear oscillator equation, going as [42,43]

$$\ddot{\phi} + \epsilon\mathcal{H}(\phi, \dot{\phi})\dot{\phi} + \frac{\mathrm{d}\mathcal{V}}{\mathrm{d}\phi} = 0, \tag{25}$$

in which $\mathcal{H}$ is a nonlinear damping coefficient (the retention of the parameter, ϵ, alongside $\mathcal{H}$, attests to its nonlinearity) and $\mathcal{V} \equiv \mathcal{V}(\phi)$, is the "potential" of the system. Going by what Eq. (23) suggests, we realize that $\mathcal{H}(\phi, \dot{\phi}) = \mathcal{A}\phi + \mathcal{B}\dot{\phi}$ and $\mathcal{V}(\phi) = \mathcal{C}(\phi^2/2) + \epsilon\mathcal{D}(\phi^3/3)$, with the constant coefficients, $\mathcal{A}$, $\mathcal{B}$, $\mathcal{C}$, and $\mathcal{D}$, having to be read from Eq. (24). The equilibrium properties resulting from Eq. (25) can be known by decomposing this second-order differential equation into a coupled first-order dynamical system. To that end, we introduce a new variable, ψ, and recast equation (25) as [43]

$$\begin{aligned}
\dot{\phi} &= \psi\\
\dot{\psi} &= -\epsilon(\mathcal{A}\phi + \mathcal{B}\psi)\psi - (\mathcal{C}\phi + \epsilon\mathcal{D}\phi^2).
\end{aligned} \tag{26}$$

Equilibrium conditions follow when $\dot{\phi} = \dot{\psi} = 0$. For the coupled dynamical system in Eq. (26), we are led to two equilibrium points on the ϕ–ψ phase plane. This is just how it should be because having accommodated nonlinearity up to the second order only Eq. (26) will be quadratic in both ϕ and ψ, yielding two equilibrium solutions. Labeling these equilibrium points with a $\star$ superscript, we see that $(\phi^\star, \psi^\star) = (0, 0)$ in one case, whereas in the other case, $(\phi^\star, \psi^\star) = (-\mathcal{C}/(\epsilon\mathcal{D}), 0)$. So, one of the equilibrium points is located at the origin of the ϕ–ψ phase plane, while the location of the other depends both on the sign and the magnitude of $\mathcal{C}/\mathcal{D}$. In effect, both of the equilibrium points lie on the line, $\psi = 0$, and correspond to the turning points of $\mathcal{V}(\phi)$. Higher orders of nonlinearity will simply proliferate equilibrium points on the line, $\psi = 0$.

Having identified the position of the two equilibriums points, our next task is to examine their stability. So we subject both equilibrium points to small perturbations and then carry out a linear stability analysis. The perturbation schemes on both ϕ and ψ are $\phi = \phi^\star + \delta\phi$ and $\psi = \psi^\star + \delta\psi$, respectively. Applying this scheme on Eq. (26) and then linearizing in $\delta\phi$ and $\delta\psi$ will yield the coupled linear dynamical system,

$$\begin{aligned}
\frac{\mathrm{d}}{\mathrm{d}t}(\delta\phi) &= \delta\psi\\
\frac{\mathrm{d}}{\mathrm{d}t}(\delta\psi) &= -\left(\left.\frac{\mathrm{d}^2\mathcal{V}}{\mathrm{d}\phi^2}\right|_{\phi=\phi^\star}\right)\delta\phi - \epsilon\mathcal{H}(\phi^\star, \psi^\star)\delta\psi,
\end{aligned} \tag{27}$$

in which $\mathrm{d}^2\mathcal{V}/\mathrm{d}\phi^2|_{\phi=\phi^\star} = \mathcal{C} + 2\epsilon\mathcal{D}\phi^\star$. Using solutions of the type, $\delta\phi \sim \exp(\omega t)$ and $\delta\psi \sim \exp(\omega t)$, in Eq. (27), the eigenvalues of the Jacobian matrix of the dynamical system follow as

$$\omega = -\epsilon\frac{\mathcal{H}}{2} \pm \sqrt{\epsilon^2\frac{\mathcal{H}^2}{4} - \left.\frac{\mathrm{d}^2\mathcal{V}}{\mathrm{d}\phi^2}\right|_{\phi=\phi^\star}}, \tag{28}$$

with $\mathcal{H} \equiv \mathcal{H}(\phi^\star, \psi^\star)$ having to be evaluated at the equilibrium points. Knowing the eigenvalues, we can classify the stability of an equilibrium point by putting its coordinates in Eq. (28). The equilibrium point at the origin has the coordinates, (0,0). Using these coordinates in Eq. (28), we get the two roots of the eigenvalues as $\omega = \pm i\sqrt{\mathcal{C}}$. If $\mathcal{C} > 0$, then the eigenvalues will be purely imaginary quantities, and consequently, the equilibrium point at the origin of the ϕ–ψ plane will be a center-type point [43]. And indeed, when the stationary inflow solution, about which the perturbation is constrained to behave like a standing wave, is subcritical over the entire region of the spatial integration, then $\mathcal{C} > 0$, because in this situation, $v_0^2 < \beta^2 c_{s0}^2$ [18].

Viewed in the ϕ–ψ phase plane, the stationary solutions about this center-type fixed point at the origin, (0,0), look like closed elliptical trajectories, much in the manner of the phase solutions of a simple harmonic oscillator with conserved total energy. More to the point, these solutions correspond entirely to the solutions with unchanging amplitudes derived from a linear stability analysis of standing waves on subsonic flows [18]. Thus, in a linear framework, a marginal sense of stability is insinuated by the center-type equilibrium point at the origin of the phase plane because solutions in its neighbourhood are purely oscillatory in time, with no change in their amplitudes. While this conclusion can be made by a linearized analysis of the standing waves [18], it could be arrived at equally correctly by setting $\epsilon = 0$ (the linear condition) in Eq. (28). An illustration of this special case is provided in Fig. 1, which traces three phase solutions of the Liénard system. One of the solutions in this plot, obtained for $\epsilon = 0$ and corresponding physically to the linear solution, is the closed elliptical trajectory about the center-type fixed point at (0,0).

Now, from dynamical systems theory, center-type points are known to be "borderline" cases [42,43]. In such situations, the linearized treatment will show marginally stable behavior, but a robust stability or an instability may emerge immediately on accounting for nonlinearity [42,43]. This can be explained by a simple but generic argument. Close to the coordinate, (0,0), Eq. (26) can be approximated in the linear form as $\dot{\phi} = \psi$ and $\dot{\psi} \simeq -\mathcal{C}\phi$, which, of course, gives a center-type point, just like a simple harmonic oscillator. Going further and accounting for the higher order nonlinear terms, Eq. (26) can be viewed as a coupled dynamical system in the form $\dot{\phi} = \mathcal{F}(\phi, \psi)$ and $\dot{\psi} = \mathcal{G}(\phi, \psi)$. Such a system is said to be "reversible" if $\mathcal{F}(\phi, -\psi) = -\mathcal{F}(\phi, \psi)$ and $\mathcal{G}(\phi, -\psi) = \mathcal{G}(\phi, \psi)$, i.e., if $\mathcal{F}$ (or $\dot{\phi}$) is an odd function of ψ and $\mathcal{G}$ (or $\dot{\psi}$) is an even function of ψ [42]. Center-type points are robust under this reversibility requirement. A look at Eq. (26) immediately reveals that $\dot{\psi}$ is not an even function of ψ. Therefore, the center-type point obtained due to a linearized analysis of Eq. (26) is a fragile one. Ample evidence of this feature can be found in the behavior of the spiraling solution in Fig. 1.

The center-type point at the origin of the phase plane has confirmed the known linear results. However, all of that is the most that a simple linear stability analysis can bring forth. With nonlinearity in its lowest order, another equilibrium point is obtained, in addition to the center-type equilibrium point. This second equilibrium point is an outcome of the quadratic order of nonlinearity in the standing wave, and its coordinates in the phase plane are $(-\mathcal{C}/(\epsilon\mathcal{D}), 0)$. Using these coordinates in Eq. (28), the eigenvalues become

$$\omega = \frac{\mathcal{A}\mathcal{C}}{2\mathcal{D}} \pm \sqrt{\left(\frac{\mathcal{A}\mathcal{C}}{2\mathcal{D}}\right)^2 + \mathcal{C}}. \tag{29}$$

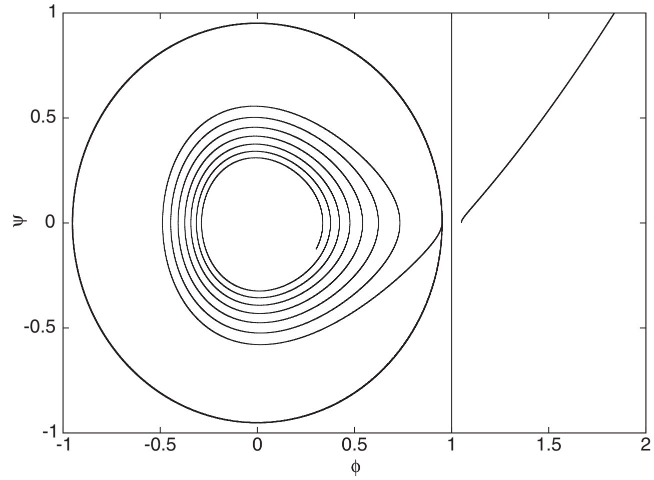

FIG. 1. With a numerical integration of Eq. (25) under chosen initial conditions, three separate phase solutions are plotted in the ϕ–ψ phase plane. The closed elliptical solution corresponds to the case of $\epsilon = 0$, with $\mathcal{C} = 1$. This is the phase solution representing the linear perturbation on standing waves, with a center-type fixed point at the origin, (0,0). The initial (ϕ, ψ) coordinates for tracing this trajectory in the phase plane are (0.95,0). Retaining the same values of $\mathcal{C}$ and the initial condition, the spiraling solution within the elliptical envelope is obtained for $\epsilon = 1$, $\mathcal{A} = \mathcal{B} = 0.03$, and $\mathcal{D} = -1$. This solution depicts the phase-plane behavior of the second-order nonlinear perturbation. With $\mathcal{C} = 1$ and $\mathcal{D} = -1$, the coordinate of the second fixed point (a saddle point) is set at (1,0). As long as the nonlinear perturbation starts with a value of $\phi < 1$ (in this case its initial value is 0.95), it will always remain close to the linear regime, and stability can be maintained. This stability is evident from the way the phase solution of the nonlinear perturbation spirals toward the center-type fixed point (which acts like an attractor). A generalization of this argument is that stability is achieved if $\phi < |\mathcal{C}/\mathcal{D}|$, and the values of $\mathcal{A}$ and $\mathcal{B}$ (whatever they may be) simply determine the rate at which the nonlinear perturbation converges toward (0,0). A strong growth of the nonlinear perturbation occurs, once its initial value exceeds the critical value of $\phi = |\mathcal{C}/\mathcal{D}|$. This critical condition is indicated by the vertical line, $\phi = 1$, near the middle of the plot. To the left of this line is the zone of stability and to its right is the zone of instability. Depending on the sign of $\mathcal{C}/\mathcal{D}$, the zone of instability will swivel either to the left or to the right of the ellipse. Setting the initial condition of the perturbation slightly to the right of $\phi = 1$, at (1.05,0), the growth of the perturbation is plainly visible, with an open trajectory diverging outward. For this diverging solution the values of ϵ, $\mathcal{A}$, $\mathcal{B}$, $\mathcal{C}$, and $\mathcal{D}$ are the same as they are for the spiraling solution to the left of $\phi = 1$.

Noting as before that $\mathcal{C} > 0$ and that $\mathcal{A}$, $\mathcal{C}$, and $\mathcal{D}$ are all real quantities, the inescapable conclusion is that the eigenvalues, ω, are also real quantities, with opposite signs. In other words, the second equilibrium point is a saddle point [43]. The position of this equilibrium point is at the coordinate $(-\mathcal{C}/\mathcal{D}, 0)$ in the ϕ–ψ phase portrait. The absolute value of the abscissa of this coordinate, $|\mathcal{C}/\mathcal{D}|$, represents a critical threshold for the initial amplitude of the perturbation. If this amplitude is less than $|\mathcal{C}/\mathcal{D}|$, then the perturbation will hover close to the linearized states about the center-type point, and stability shall prevail. The spiraling solution in Fig. 1 gives a clear demonstration of this fact. If, however, the amplitude of the perturbation exceeds the critical value, i.e., if $|\phi| > |\mathcal{C}/\mathcal{D}|$, then one enters the nonlinear regime, and in time the perturbation will undergo a divergence in one of its modes (for which ω has a positive root). This state of affairs has been depicted in the right side of the plot in Fig. 1, showing a diverging phase solution. Since the eigenvalues, ω, have been yielded on using solutions of the type, $\exp(\omega t)$, the e-folding time scale of this growing mode of the perturbation is ω^{-1}, with ω having to be read from Eq. (29).

So, in the nonlinear regime, the simple fact that emerges is that stationary subsonic global background solutions will become unstable under the influence of the perturbation. In the vicinity of a saddle point, if the initial amplitude of the perturbation is greater than $|\mathcal{C}/\mathcal{D}|$, then the solutions will continue to diverge, and higher orders of nonlinearity (starting with the third order in this case) will not smother this effect [42,43]. Since a saddle point cannot be eliminated by the inclusion of higher orders of nonlinearity [43], all that we may hope for is that the instability may grow in time until it reaches a saturation level imposed by the higher nonlinear orders (but the instability will never be decayed down). This type of instability has a precedence in the laboratory fluid problem of the hydraulic jump [54,55]. While our discussion so far has dwelt on the perturbative perspective, the saddle point also has grave consequences for evolving a critical solution in the rotational flow through the dynamic process. There can be no critical solution without gravity driving the infall process. So, from a dynamic point of view, gravity starts the evolution toward the critical state from an initial subcritical state. In the absence of any analytical prescription for the full-blown nonlinear evolution, we have tried to get as close to the nonperturbative dynamics as possible, by the inclusion of progressively higher orders of nonlinearity in our perturbative treatment. This method has revealed to us a saddle point due merely to the second order of nonlinearity. We contend that if a saddle point is to be encountered in the real-time dynamics, then there should be serious obstacles in the way of reaching a stable and stationary critical end.

VI. HIGH-FREQUENCY TRAVELING WAVES

Stability of fluids is also studied by constraining a perturbation to behave as a traveling wave. Applying the WKB approximation, some linearized studies [18,22] established the stability of inviscid rotational accretion, with the perturbation on it being a high-frequency traveling wave. With nonlinearity lending additional effects, the stability of inviscid rotational accretion merits another look. To that end, we restructure Eq. (17) using the elements, $q^{\mu\nu}$, as they are given by Eq. (19) to get

$$q^{rr}\frac{\partial^2 f'}{\partial r^2}+\left(\frac{\partial q^{tr}}{\partial t}+\frac{\partial q^{rr}}{\partial r}\right)\frac{\partial f'}{\partial r}+(q^{rt}+q^{rr})\frac{\partial^2 f'}{\partial r\partial t}+\left(\frac{\partial q^{tt}}{\partial t}+\frac{\partial q^{rt}}{\partial r}\right)\frac{\partial f'}{\partial t}+q^{tt}\frac{\partial^2 f'}{\partial t^2}=0. \tag{30}$$

The foregoing equation has lost nothing in nonlinear terms. When we set $\epsilon = 0$ in Eq. (19), the elements $q^{\mu\nu}$ render Eq. (30) linear, which can then be worked upon by a solution of the form, $f'(r,t) = R(r)\phi(t)$, with $\phi = e^{-i\omega t}$ and $R(r)$ given by a converging power series [18,22]. We show presently how this linear solution is obtained, and thereafter, we view nonlinearity as a very weak effect about the linear condition, an argument by which we continue to use $f'(r,t) = R(r)\phi(t)$ in Eq. (30) [65,66]. And since nonlinearity is now feeble, we retain only its second order in Eq. (30). What results from it eventually, after a long series of algebraic steps, is

$$\mathcal{L}_1 R + \epsilon\frac{\phi}{f_0}\mathcal{L}_2 R^2 = 0, \tag{31}$$

in which $\mathcal{L}_1$ and $\mathcal{L}_2$ are operators, given by

$$\mathcal{L}_1 \equiv (v_0^2-\beta^2 c_{s0}^2)\frac{\mathrm{d}^2}{\mathrm{d}r^2}+\left\{\frac{1}{v_0}\frac{\mathrm{d}}{\mathrm{d}r}[v_0(v_0^2-\beta^2 c_{s0}^2)]-2i\omega v_0\right\}\frac{\mathrm{d}}{\mathrm{d}r}-\left(\omega^2+2i\omega\frac{\mathrm{d}v_0}{\mathrm{d}r}\right)$$

$$\mathcal{L}_2 \equiv \frac{v_0^2}{2}\xi^{rr}\frac{\mathrm{d}^2}{\mathrm{d}r^2}+\left[\frac{1}{2v_0}\frac{\mathrm{d}}{\mathrm{d}r}(v_0^3\xi^{rr})-2i\omega v_0\xi^{tr}\right]\frac{\mathrm{d}}{\mathrm{d}r}-\left[2\xi^{tt}\omega^2+i\frac{\omega}{v_0}\frac{\mathrm{d}}{\mathrm{d}r}(v_0^2\xi^{tr})\right], \tag{32}$$

with $\mathcal{L}_1$ operating on the linear part of Eq. (31) and $\mathcal{L}_2$ on its nonlinear part. Obviously, Eq. (31) is a nonlinear ordinary differential equation in R, to solve which, we first write $R(r) = e^{s(r)}$, so that $f'(r,t) = \exp(s - i\omega t)$. With this form of R, we expand Eq. (31) as

$$(v_0^2-\beta^2 c_{s0}^2)\left[\frac{\mathrm{d}^2 s}{\mathrm{d}r^2}+\left(\frac{\mathrm{d}s}{\mathrm{d}r}\right)^2\right]+\left\{\frac{1}{v_0}\frac{\mathrm{d}}{\mathrm{d}r}[v_0(v_0^2-\beta^2 c_{s0}^2)]-2i\omega v_0\right\}\frac{\mathrm{d}s}{\mathrm{d}r}-\left(\omega^2+2i\omega\frac{\mathrm{d}v_0}{\mathrm{d}r}\right)+\epsilon\frac{R\phi}{f_0}\left\{v_0^2\xi^{rr}\left[\frac{\mathrm{d}^2 s}{\mathrm{d}r^2}+\left(\frac{\mathrm{d}s}{\mathrm{d}r}\right)^2\right]+\left[\frac{1}{v_0}\frac{\mathrm{d}}{\mathrm{d}r}(v_0^3\xi^{rr})-4i\omega v_0\xi^{tr}\right]\frac{\mathrm{d}s}{\mathrm{d}r}-\left[2\xi^{tt}\omega^2+i\frac{\omega}{v_0}\frac{\mathrm{d}}{\mathrm{d}r}(v_0^2\xi^{tr})\right]\right\}=0. \tag{33}$$

Next, we set down $s(r)$ as a power series in the form

$$s(r) = \sum_{n=-1}^{\infty} \frac{\tilde{k}_n(r)}{\omega^n}. \quad (34)$$

The principle of the WKB approximation is that successive terms in Eq. (34) follow the condition $\omega^{-n}|\tilde{k}_n(r)| \gg \omega^{-(n+1)}|\tilde{k}_{n+1}(r)|$; i.e., the power series given by $s(r)$ converges rapidly as n increases. To facilitate this outcome, we prescribe a high-frequency traveling wave, such that its wavelength, $\Lambda(r) = 2\pi(v_0 \mp \beta c_{s0})/\omega$, is much smaller than any characteristic length scale in the fluid. The smallest critical radius in the multicritical accreting system is a natural choice for such a length scale.

To find a solution of Eq. (33) a first step is to apply the WKB approximation to its linear limit, i.e., when $\epsilon = 0$. In this case, we replace all $\tilde{k}_n$ in $s(r)$ by k_n, with the latter implying the linear solution in the series of $s(r)$. After that, on making use of the series given by $s(r)$ in the linear portion of Eq. (33), we obtain the two successive highest order terms going as ω^2 and ω. Collecting all of the coefficients of ω^2, summing them up, and setting the sum equal to zero, give

$$(v_0^2 - \beta^2 c_{s0}^2)\left(\frac{\mathrm{d}k_{-1}}{\mathrm{d}r}\right)^2 - 2iv_0 \frac{\mathrm{d}k_{-1}}{\mathrm{d}r} - 1 = 0, \quad (35)$$

which is a simple quadratic that leads to

$$k_{-1} = \int \frac{i}{v_0 \mp \beta c_{s0}} \mathrm{d}r. \quad (36)$$

Working likewise with the coefficients of ω, gives

$$(v_0^2 - \beta^2 c_{s0}^2)\left(\frac{\mathrm{d}^2 k_{-1}}{\mathrm{d}r^2} + 2\frac{\mathrm{d}k_{-1}}{\mathrm{d}r}\frac{\mathrm{d}k_0}{\mathrm{d}r}\right) + \left\{\frac{1}{v_0}\frac{\mathrm{d}}{\mathrm{d}r}[v_0(v_0^2 - \beta^2 c_{s0}^2)] - 2i\omega v_0\right\}\frac{\mathrm{d}k_{-1}}{\mathrm{d}r} - 2iv_0\frac{\mathrm{d}k_0}{\mathrm{d}r} - 2i\frac{\mathrm{d}v_0}{\mathrm{d}r} = 0, \quad (37)$$

from which, on making use of Eq. (36), we extract a solution of k_0 as

$$k_0 = \ln\left(\frac{\mathrm{C}}{\sqrt{v_0 \beta c_{s0}}}\right), \quad (38)$$

with C being a constant of integration. Both k_{-1} and k_0 give the two leading terms in the series of $s(r)$. From Eqs. (36) and (38), respectively, these terms go asymptotically as $k_{-1} \sim r$ and $k_0 \sim \ln r$, given the condition that $v_0 \sim r^{-5/2}$ on large length scales, while c_{s0} approaches its constant ambient value. The next term in the series, k_1, behaves asymptotically as $k_1 \sim r^{-1}$. So, under the regime of a high-frequency traveling wave, all of this implies $\omega|k_{-1}| \gg |k_0| \gg \omega^{-1}|k_1|$. Therefore, it suffices to consider the two leading terms only, involving k_{-1} and k_0 in the series expansion of $s(r)$.

Equations (36) and (38) give the leading linear solution of Eq. (33) when $\epsilon = 0$. To incorporate the effect of nonlinearity, i.e., when $\epsilon \neq 0$, we employ an iterative technique on Eq. (33) and collect the nonlinear contribution to ω^2 and ω only. We achieve this through the following logical sequence, remembering that nonlinearity is a small effect about the linear solution.

(i) In Eq. (33), the nonlinear ϵ-dependent part carries the time-dependent factor, $\phi = e^{-i\omega t}$. We expand it as a power series in $-i\omega t$, going as $\phi(t) = 1 - i\omega t + (-i\omega t)^2/2! + \cdots$ and apply a truncation immediately after the zeroth-order term. Otherwise, retention of any order higher than unity will allow the series to make a time-dependent contribution to R in violation of the restriction that $R(r)$ has to self-consistently bear only a spatial dependence in the feebly nonlinear regime.

(ii) In the ϵ-dependent part of Eq. (33), we replace all nonlinear $\tilde{k}_n$ by the linear k_n, in accordance with our iterative principle, with a truncation applied immediately after k_0.

(iii) Thereafter, in the ϵ-dependent part of Eq. (33), the function, $R(r)$, is to be read as, $R(r) \simeq \exp(\omega k_{-1} + k_0)$, which we finally expand to $R(r) \simeq \mathrm{C}(v_0 \beta c_{s0})^{-1/2} (1 + \omega k_{-1} + \omega^2 k_{-1}^2/2!)$. We have truncated the series expansion beyond the second order because the higher orders will be irrelevant for the $\tilde{k}_n$ series, insofar as our objective is to determine the contribution of nonlinearity only to the terms carrying ω^2 and ω.

Now, with the involvement of nonlinearity, the sum of the coefficients of ω^2 in Eq. (33), set to zero, will read as

$$(v_0^2 - \beta^2 c_{s0}^2)\left(\frac{\mathrm{d}\tilde{k}_{-1}}{\mathrm{d}r}\right)^2 - 2iv_0\frac{\mathrm{d}\tilde{k}_{-1}}{\mathrm{d}r} - (1 - \epsilon\mathcal{P}) = 0, \quad (39)$$

in which,

$$\mathcal{P} = \frac{\mathrm{C}}{f_0\sqrt{v_0 \beta c_{s0}}}\left(\mathcal{X} + \mathcal{Y}k_{-1} + \frac{1}{2}\mathcal{Z}k_{-1}^2\right), \quad (40)$$

and further,

$$\mathcal{X} = 2v_0^2 \xi^{rr}\left(\frac{\mathrm{d}k_{-1}}{\mathrm{d}r}\right)^2 - 4iv_0\xi^{tr}\frac{\mathrm{d}k_{-1}}{\mathrm{d}r} - 2\xi^{tt},$$

$$\mathcal{Y} = v_0^2\xi^{rr}\left(4\frac{\mathrm{d}k_0}{\mathrm{d}r}\frac{\mathrm{d}k_{-1}}{\mathrm{d}r} + \frac{\mathrm{d}^2 k_{-1}}{\mathrm{d}r^2}\right) + \frac{1}{v_0}\frac{\mathrm{d}}{\mathrm{d}r}(v_0^3\xi^{rr})\frac{\mathrm{d}k_{-1}}{\mathrm{d}r} - 4iv_0\xi^{tr}\frac{\mathrm{d}k_0}{\mathrm{d}r} - \frac{i}{v_0}\frac{\mathrm{d}}{\mathrm{d}r}(v_0^2\xi^{tr}),$$

$$\mathcal{Z} = v_0^2\xi^{rr}\left[\frac{\mathrm{d}^2 k_0}{\mathrm{d}r^2} + 2\left(\frac{\mathrm{d}k_0}{\mathrm{d}r}\right)^2\right] + \frac{1}{v_0}\frac{\mathrm{d}}{\mathrm{d}r}(v_0^3\xi^{rr})\frac{\mathrm{d}k_0}{\mathrm{d}r}. \quad (41)$$

The coefficients $\mathcal{X}$ and $\mathcal{Z}$ are real, while $\mathcal{Y}$ is imaginary, from all of which $\mathcal{P}$ can be seen to be real. On treating nonlinearity as a small effect and performing a binomial expansion, we obtain the solution of Eq. (39) as

$$\tilde{k}_{-1} = k_{-1} \pm \epsilon \frac{i}{2} \int \frac{\mathcal{P}}{\beta c_{s0}} \mathrm{d}r. \tag{42}$$

Since $\mathcal{P}$ is a real quantity, the contribution of nonlinearity in $\tilde{k}_{-1}$ goes only to the phase part of $f'(r,t)$.

Similarly, the coefficients of ω, from Eq. (33), give

$$\begin{aligned}(v_0^2 - \beta^2 c_{s0}^2)\left(\frac{\mathrm{d}^2\tilde{k}_{-1}}{\mathrm{d}r^2} + 2\frac{\mathrm{d}\tilde{k}_{-1}}{\mathrm{d}r}\frac{\mathrm{d}\tilde{k}_0}{\mathrm{d}r}\right) \\ + \left\{\frac{1}{v_0}\frac{\mathrm{d}}{\mathrm{d}r}[v_0(v_0^2 - \beta^2 c_{s0}^2)] - 2i\omega v_0\right\}\frac{\mathrm{d}\tilde{k}_{-1}}{\mathrm{d}r} - 2iv_0\frac{\mathrm{d}\tilde{k}_0}{\mathrm{d}r} \\ - 2i\frac{\mathrm{d}v_0}{\mathrm{d}r} + \epsilon\frac{\mathrm{C}}{f_0\sqrt{v_0\beta c_{s0}}}(\mathcal{Y} + \mathcal{Z}k_{-1}) = 0,\end{aligned} \tag{43}$$

from which, with the aid of Eq. (42) and a binomial expansion for weak nonlinearity, we extract a solution of $\tilde{k}_0$ as

$$\tilde{k}_0 = k_0 - \epsilon\frac{\mathcal{P}}{4}(\mathrm{M}^2 - 1) \pm \epsilon \int \frac{\mathcal{Q}}{2v_0\beta c_{s0}} \mathrm{d}r, \tag{44}$$

where the scaled Mach number $\mathrm{M} = v_0/\beta c_{s0}$ and

$$\mathcal{Q} = iv_0 \frac{\mathrm{C}}{f_0\sqrt{v_0\beta c_{s0}}}(\mathcal{Y} + \mathcal{Z}k_{-1}). \tag{45}$$

Since $\mathcal{Y}$ is imaginary and $\mathcal{Z}$ is real, $\mathcal{Q}$ is also real, which means that the nonlinear contribution to $\tilde{k}_0$ goes to the amplitude of $f'(r,t)$. In terms of $\tilde{k}_{-1}$ and $\tilde{k}_0$, the two most dominant contributors to $s(r)$, we write the perturbation in a slightly altered form as $f'(r,t) \simeq e^{\tilde{k}_0}\exp(\omega\tilde{k}_{-1} - i\omega t)$. This perturbation should be viewed as a superposition of two traveling waves. Both of these waves move with the speed, βc_{s0}, relative to the fluid, one against the bulk flow and the other along with it, while the bulk flow itself has the velocity, v_0. The amplitude of the perturbation is determined only by $\tilde{k}_0$, which we extract as

$$|f'(r,t)| \simeq \frac{\mathrm{C}}{\sqrt{v_0\beta c_{s0}}}\exp\left[\epsilon\frac{\mathcal{P}}{4}(1 - \mathrm{M}^2) \pm \epsilon\int\frac{\mathcal{Q}}{2v_0\beta c_{s0}}\mathrm{d}r\right]. \tag{46}$$

The effect of nonlinearity manifests itself in the high-frequency traveling wave in two ways. First, the $\mathcal{P}$-dependent term in Eq. (46) will exhibit divergence, depending on the sign of $\mathcal{P}$. If $\mathcal{P} < 0$, then there will be a divergence in the supercritical region of the flow, where $\mathrm{M} > 1$. If $\mathcal{P} > 0$, then the divergence will be in the subcritical zone, where $\mathrm{M} < 1$. It appears that the acoustic horizon plays a crucial role in segregating the two regions, in one of which the perturbation will experience growth. Second, the $\mathcal{Q}$-dependent term in Eq. (46) also contributes a growth mode (the one with the positive sign) to the amplitude of the perturbation. In short, just as it was seen in the case of the standing waves, nonlinearity also causes an instability in the high-frequency traveling waves.

We see this feature in the energy flux of the traveling waves as well. The kinetic energy contained in a unit volume of fluid is

$$\mathcal{E}_{\mathrm{kin}} = \frac{1}{2}(\rho_0 + \rho')(v_0 + v')^2. \tag{47}$$

The potential energy per unit volume of the fluid is the sum of its internal energy, the gravitational energy, and the rotational energy, all of which are expressed together as

$$\begin{aligned}\mathcal{E}_{\mathrm{pot}} = (\rho_0 + \rho')\Phi - (\rho_0 + \rho')\frac{\lambda^2}{2r^2} + \rho_0\varepsilon + \rho'\frac{\partial}{\partial\rho_0}(\rho_0\varepsilon) \\ + \frac{1}{2}\rho'^2\frac{\partial^2}{\partial\rho_0^2}(\rho_0\varepsilon),\end{aligned} \tag{48}$$

where ε is the internal energy per unit mass [36]. In Eqs. (47) and (48), the zeroth-order terms refer to the background flow. The first-order terms vanish on time averaging, and the principal contribution to the time-averaged total energy in the perturbation comes from the second-order terms. Together they yield

$$\mathcal{E}_{\mathrm{tot}} = \frac{1}{2}\rho_0 v'^2 + v_0\rho' v' + \frac{1}{2}\rho'^2\frac{\partial^2}{\partial\rho_0^2}(\rho_0\varepsilon). \tag{49}$$

If the perturbation is adiabatic, then the condition, $\mathrm{d}S = 0$, in the thermodynamic relation, $\mathrm{d}\varepsilon = T\mathrm{d}S + (P/\rho^2)\mathrm{d}\rho$, gives

$$\left.\frac{\partial^2}{\partial\rho_0^2}(\rho_0\varepsilon)\right|_S = \frac{c_{s0}^2}{\rho_0}. \tag{50}$$

Our next task is to represent both ρ' and v' in terms of f' in Eq. (49), after which, f' itself is to be substituted with the help of Eq. (46). So, referring to Eq. (8), and considering it in the linear order, i.e., with $\zeta = 1$, we get

$$\frac{1}{\beta^2}\frac{\rho'}{\rho_0} \simeq \frac{v_0}{v_0 \mp \beta c_{s0}}\frac{f'}{f_0}. \tag{51}$$

We note that the foregoing result is precisely what Eq. (18) implies. Further, making use of Eq. (51) in Eq. (6), with $\zeta = 1$ and ignoring the product of ρ' and v' in the latter, gives us

$$\frac{v'}{v_0} \simeq \mp \frac{\beta c_{s0}}{v_0 \mp \beta c_{s0}} \frac{f'}{f_0}. \tag{52}$$

Combining the results provided by Eqs. (51) and (52), with Eq. (46), we get the time-averaged total energy of the perturbation per unit volume as

$$\mathcal{E}_{\rm tot} \simeq \frac{1}{2}\frac{\beta^2 C^2}{f_0^2}\frac{v_0\rho_0}{(v_0 \mp \beta c_{s0})^2}\left[\frac{\beta c_{s0}}{2}\left(1+\frac{1}{\beta^2}\right) \mp v_0\right] \times \exp\left[\epsilon\frac{\mathcal{P}}{2}(1-M^2) \pm \epsilon\int\frac{\mathcal{Q}}{v_0\beta c_{s0}}dr\right], \tag{53}$$

with the factor of $1/2$ arising from the time averaging of the phase part of f'^2. We obtain the energy flux of the cylindrical wavefront by multiplying $\mathcal{E}_{\rm tot}$ by the propagation velocity $(v_0 \mp \beta c_{s0})$ and then by integrating over the area of the cylindrical face of the disc distribution, which is $2\pi r H$. Substituting H from Eq. (2), together with the condition that $H \ll r$, we derive an expression for the energy flux as

$$F = \frac{2\pi C^2\sqrt{k}}{f_0(\gamma+1)}\left[\mp 1 + \frac{\gamma-1}{4(M \mp 1)}\right] \times \exp\left[\epsilon\frac{\mathcal{P}}{2}(1-M^2) \pm \epsilon\int\frac{\mathcal{Q}}{v_0\beta c_{s0}}dr\right]. \tag{54}$$

The ϵ-dependent factor causes a growth behavior in the energy flux of the traveling wave, in the same way as it does to its amplitude. Also, when $M = 1$, the wave propagating against the bulk flow, apparently suffers a divergence, but the case for stability in this instance is already made [22]. So the instability is owed only to nonlinear effects.

VII. CONCLUDING REMARKS

Much of the analytical methods of our work have closely followed those of a similar study on spherically symmetric accretion [62]. Considering the difference between the respective geometries of spherically symmetric accretion and axisymmetric accretion, as well as differences in the respective physics, the emergence of the same mathematical structure in both the cases is intriguing and perhaps hints at something of a universal nature, where nonlinearity in fluid flows is concerned.

The Liénard system derived in our work indicates that the number of equilibrium points depends on the order of nonlinearity that is retained in the equation of the perturbation. Additional equilibrium points, resulting from higher orders of nonlinearity, may temper the instability that has been found here. However, up to the second order at least, an instability in real time appears undeniable. The WKB analysis of a traveling-wave perturbation leads to the same conclusion. Perhaps this instability is connected to the constant distribution of angular momentum, a result known in rotational accretion of perfect fluids (see [67] and references therein). In the analogous case of an inviscid and incompressible Couette flow, which also has an axial symmetry, Rayleigh's criterion for stability states that the stratification of angular momentum in the flow is stable if and only if it increases monotonically outward, i.e., has a positive gradient [68]. If, however, the gradient of the angular momentum is negative, then the rotational flow will be unstable. To carry this analogy over to the inviscid accretion disc, the gradient of the constant distribution of angular momentum is zero. So effectively this implies a borderline case between a stable positive gradient and an unstable negative gradient. Such borderline cases may show apparently stable features under a linearized analysis, but in these situations, it is always safer to draw conclusions regarding stability only from a nonlinear analysis, as the spiraling and the diverging solutions in Fig. 1 show. There are other disc models, in which angular momentum maintains a positive gradient, as, for example, the Keplerian accretion disc [1]. Examining the stability of such configurations may lead to a clear view of the connection between the stability of axisymmetric accretion and the distribution of angular momentum.

A natural attribute of real fluids is viscosity. Fluid flows are affected both by nonlinearity and viscosity, occasionally as competing effects. In models of accretion discs, viscous dissipation usually brings about stability, but in one of the models of axisymmetric accretion, namely, the quasiviscous accretion disc, viscosity actually destabilizes the flow under linear perturbations [41,45]. In this model, kinematic viscosity is constrained as a vanishingly small first-order perturbative effect about a background inviscid flow. This instability, known as secular instability, is not without its precedence. Exactly this kind of instability is also seen to grow in Maclaurin spheroids on the introduction of a kinematic viscosity to a first order [69]. There may, however, be an advantage in this secular instability, which is most pronounced on large length scales of an accretion disc [41]. No inflow solution, starting from the outer spatial limits of the accretion process, can be free of time dependence because of the secular instability. Now, since a viscous disc gets spatially distributed on the viscous time scale, the time-dependent behavior of solutions can be exploited to understand the nature of viscosity, especially since observables in a steady disc are largely independent of viscosity [1]. The perturbative methods of our work (which takes nonlinearity up to the second order) can be combined with the aforementioned quasiviscous model (which takes viscosity to a small linear order), with the result that nonlinearity will augment the linear-order secular instability brought about by viscosity. Since the molecular viscosity of the inflowing gas is very weak [1], strongly time-dependent behavior of solutions may carry the signature of the nonlinear character of the flow.

ACKNOWLEDGMENTS

This research has made use of NASA's Astrophysics Data System. This work was done under the National Initiative on Undergraduate Science (NIUS), conducted by Homi Bhabha Centre for Science Education, the Tata Institute of Fundamental Research, Mumbai, India. The authors express gratitude to J. K. Bhattacharjee, T. K. Das, T. Naskar, and S. Roy Chowdhury for useful comments and A. R. Dhakulkar and A. Mazumdar for help in various academic matters.

[1] J. Frank, A. King, and D. Raine, *Accretion Power in Astrophysics* (Cambridge University Press, Cambridge, England, 2002).
[2] B. Paczyński and P. J. Wiita, Astron. Astrophys. **88**, 23 (1980).
[3] A. M. Nowak and R. V. Wagoner, Astrophys. J. **378**, 656 (1991).
[4] I. V. Artemova, G. Björnsson, and I. D. Novikov, Astrophys. J. **461**, 565 (1996).
[5] Z. Stuchlík and J. Kovář, Int. J. Mod. Phys. D **17**, 2089 (2008).
[6] B. Carter, *Active Galactic Nuclei*, edited by C. Hazard and S. Mitton (Cambridge University Press, Cambridge, England, 1979).
[7] E. P. T. Liang and K. A. Thomson, Astrophys. J. **240**, 271 (1980).
[8] M. A. Abramowicz and W. H. Zurek, Astrophys. J. **246**, 314 (1981).
[9] S. K. Chakrabarti, Astrophys. J. **347**, 365 (1989).
[10] K. Nakayama and J. Fukue, Publ. Astron. Soc. Jpn. **41**, 271 (1989).
[11] S. K. Chakrabarti, *Theory of Transonic Astrophysical Flows* (World Scientific, Singapore, 1990).
[12] R. X. Yang and M. Kafatos, Astron. Astrophys. **295**, 238 (1995).
[13] V. I. Pariev, Mon. Not. R. Astron. Soc. **283**, 1264 (1996).
[14] S. K. Chakrabarti, Phys. Rep. **266**, 229 (1996).
[15] J. F. Lu, K. N. Yu, F. Yuan, and E. C. M. Young, Astron. Astrophys. **321**, 665 (1997).
[16] T. K. Das, Astrophys. J. **577**, 880 (2002).
[17] T. K. Das, J. K. Pendharkar, and S. Mitra, Astrophys. J. **592**, 1078 (2003).
[18] A. K. Ray, Mon. Not. R. Astron. Soc. **344**, 83 (2003).
[19] P. Barai, T. K. Das, and P. J. Wiita, Astrophys. J. **613**, L49 (2004).
[20] T. K. Das, Mon. Not. R. Astron. Soc. **349**, 375 (2004).
[21] H. Abraham, N. Bilić, and T. K. Das, Classical Quantum Gravity **23**, 2371 (2006).
[22] S. Chaudhury, A. K. Ray, and T. K. Das, Mon. Not. R. Astron. Soc. **373**, 146 (2006).
[23] A. K. Ray and J. K. Bhattacharjee, Classical Quantum Gravity **24**, 1479 (2007).
[24] S. Goswami, S. N. Khan, A. K. Ray, and T. K. Das, Mon. Not. R. Astron. Soc. **378**, 1407 (2007).
[25] T. K. Das, N. Bilić, and S. Dasgupta, J. Cosmol. Astropart. Phys. 6 (2007) 009.
[26] N. Roy and A. K. Ray, Mon. Not. R. Astron. Soc. **397**, 1374 (2009).
[27] S. Nag, S. Acharya, A. K. Ray, and T. K. Das, New Astron. **17**, 285 (2012).
[28] I. V. Igumenshchev and A. M. Beloborodov, Mon. Not. R. Astron. Soc. **284**, 767 (1997).
[29] A. M. Beloborodov and A. F. Illarionov, Mon. Not. R. Astron. Soc. **323**, 167 (2001).
[30] D. Proga and M. C. Begelman, Astrophys. J. **582**, 69 (2003).
[31] A. F. Illarionov and R. A. Sunyaev, Astron. Astrophys. **39**, 185 (1975).
[32] E. P. Liang and P. L. Nolan, Space Sci. Rev. **38**, 353 (1984).
[33] D. V. Bisikalo, A. A. Boyarchuk, V. M. Chechetkin, O. A. Kuznetsov, and D. Molteni, Mon. Not. R. Astron. Soc. **300**, 39 (1998).
[34] A. F. Illarionov, Sov. Astron. **31**, 618 (1987).
[35] I. V. Igumenshchev and M. A. Abramowicz, Mon. Not. R. Astron. Soc. **303**, 309 (1999).
[36] L. D. Landau and E. M. Lifshitz, *Fluid Mechanics* (Butterworth-Heinemann, Oxford, 1987).
[37] I. D. Novikov and K. S. Thorne, *Black Holes: Les Houches*, edited by C. DeWitt (Gordon & Breach, New York, 1973).
[38] S. L. Shapiro and S. A. Teukolsky, *Black Holes, White Dwarfs and Neutron Stars* (Wiley, New York, 1983).
[39] B. Muchotrzeb-Czerny, Acta Astronomica **36**, 1 (1986).
[40] N. Afshordi and B. Paczyński, Astrophys. J. **592**, 354 (2003).
[41] J. K. Bhattacharjee, A. Bhattacharya, T. K. Das, and A. K. Ray, Mon. Not. R. Astron. Soc. **398**, 841 (2009).
[42] S. H. Strogatz, *Nonlinear Dynamics and Chaos* (Addison-Wesley Publishing Company, Reading, MA, 1994).
[43] D. W. Jordan and P. Smith, *Nonlinear Ordinary Differential Equations* (Oxford University Press, Oxford, 1999).
[44] A. K. Ray and J. K. Bhattacharjee, Phys. Rev. E **66**, 066303 (2002).
[45] J. K. Bhattacharjee and A. K. Ray, Astrophys. J. **668**, 409 (2007).
[46] W. Unruh, Phys. Rev. Lett. **46**, 1351 (1981).
[47] T. Jacobson, Phys. Rev. D **44**, 1731 (1991).
[48] W. Unruh, Phys. Rev. D **51**, 2827 (1995).
[49] M. Visser, Classical Quantum Gravity **15**, 1767 (1998).
[50] N. Bilić, Classical Quantum Gravity **16**, 3953 (1999).
[51] R. Schützhold and W. Unruh, Phys. Rev. D **66**, 044019 (2002).
[52] S. B. Singha, J. K. Bhattacharjee, and A. K. Ray, Eur. Phys. J. B **48**, 417 (2005).
[53] G. Volovik, JETP Lett. **82**, 624 (2005).
[54] G. Volovik, J. Low Temp. Phys. **145**, 337 (2006).
[55] A. K. Ray and J. K. Bhattacharjee, Phys. Lett. A **371**, 241 (2007).

[56] N. Roy and A. K. Ray, Mon. Not. R. Astron. Soc. **380**, 733 (2007).

[57] T. Naskar, N. Chakravarty, J. K. Bhattacharjee, and A. K. Ray, Phys. Rev. D **76**, 123002 (2007).

[58] P. Mach and E. Malec, Phys. Rev. D **78**, 124016 (2008).

[59] C. Barceló, S. Liberati, and M. Visser, Living Rev. Relativity **14**, 3 (2011).

[60] S. J. Robertson, J. Phys. B **45**, 163001 (2012).

[61] N. Sarkar, A. Basu, J. K. Bhattacharjee, and A. K. Ray, Phys. Rev. C **88**, 055205 (2013).

[62] S. Sen and A. K. Ray, Phys. Rev. D **89**, 063004 (2014).

[63] S. Chandrasekhar, *An Introduction to the Study of Stellar Structure* (University of Chicago Press, Chicago, 1939).

[64] F. K. Shu, *The Physics of Astrophysics, Vol. II: Gas Dynamics* (University Science Books, California, 1991).

[65] A. D. Polyanin and V. F. Zaitsev, *Handbook of Nonlinear Partial Differential Equations* (Chapman and Hall/CRC, Boca Raton, FL, 2004).

[66] T. J. Bridges and F. E. Laine-Pearson, SIAM J. Appl. Math. **64**, 2096 (2004).

[67] L. Rezzolla, S. Yoshida, and O. Zanotti, Mon. Not. R. Astron. Soc. **344**, 978 (2003).

[68] S. Chandrasekhar, *Hydrodynamic and Hydromagnetic Stability* (Dover Publications, New York, 1981).

[69] S. Chandrasekhar, *Ellipsoidal Figures of Equilibrium* (Dover Publications, New York, 1987).